

Structure and dynamics of nonaqueous mixtures of dipolar liquids. II. Molecular dynamics simulations

Dean S. Venables and Charles A. Schmuttenmaer

Department of Chemistry, Yale University, 225 Prospect Street, P.O. Box 208107, New Haven, Connecticut 06520-8107

(Received 13 March 2000; accepted 24 May 2000)

Molecular dynamics simulations have been used to study mixtures of acetone/methanol, acetonitrile/methanol, and acetone/acetonitrile over their entire composition range. Using the effective pair potentials of the neat liquids, the simulations reproduce much of the experimental spectra presented in the previous paper [D. S. Venables, A. Chiu, and C. A. Schmuttenmaer, *J. Chem. Phys.* **113**, 3243 (2000)]. In addition to the total dipole spectra, autocorrelation functions and their corresponding spectra were calculated for the single dipole moment as well as the translational and rotational velocities of each component in the mixtures. Radial and spatial distribution functions, hydrogen bonding, and methanol chain formation in the mixtures were also analyzed. The red-shift of the high frequency librational band is attributed to methanol chains breaking up into shorter segments, and to hydrogen bonding between methanol and co-solvent molecules. Methanol molecules have a strong tendency to reside in chains, even at low methanol concentrations, and hydrogen bonding is the primary determinant of structure in the mixtures. © 2000 American Institute of Physics. [S0021-9606(00)51432-9]

I. INTRODUCTION

In the preceding paper,¹ we discussed how a combination of experimental intermolecular spectra and molecular dynamics (MD) simulations is needed to arrive at a detailed understanding of the dynamics of liquids. The combination of experimental and simulation techniques is a two-way procedure: the experimental spectra are required to evaluate the accuracy of the simulations, which serve in turn to interpret the experimental spectra. Our focus in these two papers is on the nonaqueous dipolar liquid mixtures of acetone/methanol, acetonitrile/methanol, and acetone/acetonitrile. In the preceding paper, we measured the experimental infrared spectra of these mixtures below 120 cm^{-1} , and from 400 to 1000 cm^{-1} for the methanolic mixtures.¹ We observed that the low frequency spectra of all the mixtures behave ideally (in contrast to aqueous mixtures at these frequencies). However, at high frequencies there is a dramatic change in the librational band of the methanol molecules as co-solvent is added. In this paper, we report the results of MD simulations of these mixtures.

Computer simulation has proven to be an indispensable tool for investigating the behavior of liquids. Simulations have successfully reproduced many of the macroscopic and microscopic properties of liquids.² In particular, MD simulations allow us to probe both the structure and the dynamics of the system in unprecedented detail. The interaction potentials of liquids used in simulations are optimized to describe the experimental properties of neat liquids. It does not necessarily follow that the same models will also describe the behavior of mixtures satisfactorily. Before we can infer details about molecular behavior with confidence, we must first verify that simulations reproduce experimental results. However, we are not aware of any studies comparing the experi-

mental intermolecular spectra of dipolar mixtures to spectra calculated using MD simulations.

Our purpose in this study is to use MD simulations to interpret the experimental spectra of acetone/methanol, acetonitrile/methanol, and acetone/acetonitrile mixtures that were reported in the preceding paper. MD simulations of the same mixtures were performed to calculate dynamic properties related to the spectra. The structure and dynamics of the mixtures, particularly the effects of hydrogen bonding, will be examined. Since we find good agreement between the simulations and experiment, we are able to extract information about the microscopic behavior of the mixtures from the simulations.

II. BACKGROUND

Methanol, acetone, and acetonitrile have each been investigated in a number of MD studies. In methanol, the OPLS model of Jorgensen³ and the H1 model of Haughney, Ferrario, and McDonald⁴ show good agreement with experimental values for thermodynamic, structural, and dynamic properties. Simulations using these models show that most methanol molecules simultaneously donate and accept a hydrogen bond. Consequently, liquid methanol consists of long, winding chains of molecules. About 7% of methanol molecules accept more than one hydrogen bond, thereby allowing branching in the chains. The distribution of chains of various lengths in the simulation has been calculated by Matsumoto and Gubbins.⁵ They found that the number of chains drops rapidly as the chain length increases, although large chains of over 100 molecules were sometimes observed. In neat methanol, the mean number of molecules per chain was 15.5 at room temperature. Molecules involved in two hydrogen bonds remained in the same bonding state for much

longer than did nonbonded molecules, chain end molecules (one hydrogen bond), and branching molecules (three hydrogen bonds). Martí *et al.* found that the translational motions of methanol molecules with two or three hydrogen bonds had more high frequency spectral density than did molecules with zero or one hydrogen bonds.⁶

Skaf, Fonseca, and Ladanyi have studied the effect of incorporating induced dipoles on the methanol dielectric relaxation.⁷ The permanent dipole is the largest contributor to the dielectric relaxation. Although the contribution of the induced dipoles to the dielectric relaxation is nonnegligible, for the most part it relaxes at the same rate as the permanent dipole. Consequently, reorientational motion is responsible for most of the far-IR spectrum, and collision-induced dipoles lower the absorption of the sample slightly at higher frequencies. Their spectra showed three peaks, at 60 cm⁻¹, 150 cm⁻¹, and 645 cm⁻¹. The high frequency absorption band was attributed to libration of the hydroxyl H around the CO bond axis.

Polarizable⁸ and nonpolarizable^{9,10} models have been proposed for simulations of acetone. Jedlovsky and Pálinskás reported that the structure of acetone is influenced more by steric effects than by electrostatic forces.⁸ The CO bond vectors of nearest neighbors in the liquid tend to be oriented in an antiparallel manner, but other molecules in the first coordination shell have no preferred orientation. In contrast, dipole-dipole interactions are much stronger in acetonitrile and in consequence it is a more structured liquid.¹¹⁻¹³ Radial distribution functions (RDFs) show that acetonitrile molecules often align in a head-to-tail configuration, while laterally displaced neighbors tend to adopt an antiparallel arrangement.

Representative simulations of *mixtures* can be found in Refs. 9 and 14-19. In the work reported here, the potentials between like interaction sites were the same as those of the neat liquids, which are based on the Lennard-Jones potential: $U(r) = 4\epsilon[(\sigma/r)^{12} - (\sigma/r)^6]$. The potentials between unlike sites i and j were determined using the Lorentz-Berthelot combining rules:²⁰ $\sigma_{ij} = (\sigma_i + \sigma_j)/2$ and $\epsilon_{ij} = \sqrt{\epsilon_i \epsilon_j}$. Although the potentials were optimized to describe the properties of the neat liquids, the above approach has produced reasonable agreement with experiment (for example, see Refs. 2, 9, 15). In particular, the simulations reproduce how dynamic properties such as the diffusion coefficient change as a function of composition.

As befits their importance, aqueous mixtures have received considerably more attention than other mixtures. Because methanol bears a similarity to water in that it is also a highly associating liquid, some general results of mixing in water will be presented below. The results presented in this paper show that some of the trends observed in aqueous mixtures occur in methanolic mixtures too.

The addition of a co-solvent to water produces a marked increase in the RDFs associated with hydrogen bonding between water molecules, such as the O-O and O-H RDFs.^{9,16,21-23} This indicates that water molecules have a strong tendency toward self-association in the mixture.^{16,24} The increase in water-water RDFs has also been attributed to an increase in the water structure in the mixture.^{9,14,16} A

TABLE I. Lennard-Jones potential function parameters of the neat liquids (Refs. 3, 10, 11). Geometries of the molecules are taken from the same references, and from Ref. 30 for acetone.

Site	q (e)	σ (\AA)	ϵ (kJ mol^{-1})
Methanol			
CH ₃	0.265	3.775	0.866
O	-0.700	3.070	0.711
H	0.435
Acetone			
CH ₃	0.062	3.910	0.669
C	0.300	3.750	0.439
O	-0.424	2.960	0.879
Acetonitrile			
CH ₃	0.150	3.775	0.866
C	0.280	3.650	0.628
N	-0.430	3.200	0.711

significant slowing of the dynamics of the water molecules upon mixing has been observed. Water molecules in mixtures have smaller diffusion coefficients than in the neat liquid, reorientational correlation times are longer, and Debye relaxation times are longer.²⁵

Pronounced changes in the high frequency librational band of water have been observed with mixing. This absorption band is particularly interesting, as it reflects the motions of the hydrogen atoms, and hence is sensitive to the hydrogen bonding environment. In mixtures with a polar cosolvent (e.g., methanol,^{9,26} DMSO,^{18,19} formamide,¹⁵ and acetonitrile¹⁶), the high frequency librational band of water may split into two or may move to higher or lower frequencies. Addition of nonpolar cosolvents tends to shift the band to higher frequencies.^{14,17} As mentioned above, we are not aware of any experimental corroboration of these predictions regarding the librational dynamics. In earlier and on-going work, we observed that there are large nonidealities in the experimental low frequency (below 100 cm⁻¹) infrared spectra of aqueous mixtures.^{25,27} The marked changes in the properties of aqueous mixtures are not mirrored in nonassociating liquids.²⁸

III. EXPERIMENT

Constant volume MD simulations were carried out using the MolDy program.²⁹ Systems of 216 rigid molecules were simulated at an average temperature of 298 K using periodic boundary conditions and an integration time step of 0.7 fs. The effective pair potentials used in the simulations were OPLS for methanol³ and for acetone,^{10,30} and Jorgenson-Briggs for acetonitrile.¹¹ The parameters are listed in Table I. Long-range electrostatic interactions were accounted for by Ewald summation. The system was equilibrated for 70 ps, followed by a 126 ps period during which data were collected. Dynamic quantities for the time correlation functions were output every 7 ps. Experimental densities were measured at about 293 K, and were scaled so that the densities of the neat liquids corresponded to the literature values at 298

TABLE II. Values of the densities and number of molecules used in simulations of the mixtures. The number of molecules and the corresponding volume fraction refers to the first component of the mixture. (AT designates acetone and AN designates acetonitrile.)

Acetone/Methanol			Acetonitrile/Methanol			Acetone/Acetonitrile		
# AT	Density (g cm ⁻³)	V _{AT}	# AN	Density (g cm ⁻³)	V _{AN}	# AT	Density (g cm ⁻³)	V _{AT}
0	0.7872	0.0000	0	0.7872	0.0000	0	0.7793	0.0000
13	0.7884	0.1042	17	0.7872	0.0996	16	0.7788	0.1009
36	0.7902	0.2665	45	0.7874	0.2541	42	0.7803	0.2531
84	0.7917	0.5362	96	0.7860	0.5087	92	0.7827	0.5101
144	0.7907	0.7842	153	0.7827	0.7586	150	0.7845	0.7613
186	0.7881	0.9184	190	0.7803	0.9044	189	0.7850	0.9076
216	0.7856	1.0000	216	0.7793	1.0000	216	0.7856	1.0000

K.³¹ The densities, volume fractions, and number of molecules in each simulation are listed in Table II. Preliminary studies showed that using other common potentials for the liquids did not significantly influence the resulting spectra. As in the preceding paper, we denote the volume fraction of component i with the symbol V_i . Where appropriate, mole fractions are used and are designated by the conventional symbol, x_i . The component i may be written as AT for acetone, AN for acetonitrile, or ME for methanol.

The far-IR spectra of the simulated liquids were calculated from the autocorrelation function (ACF) of the total dipole moment, $\mathbf{M}(t)$, using the equation:

$$\alpha(\omega)n(\omega) = \frac{4\pi\omega \tanh(\hbar\omega/2kT)}{3\hbar cV} \times \int_{-\infty}^{+\infty} e^{-i\omega t} \langle \mathbf{M}(t) \cdot \mathbf{M}(0) \rangle dt, \quad (1)$$

where α is the absorption coefficient and n is the index of refraction of a sample of volume, V , and temperature, T .³² The absorption coefficient and index of refraction were separated using a Kramers–Kronig analysis.^{33,34}

In this work, the total dipole was calculated based solely on the permanent dipole of each molecule; induced dipoles were not taken into account. This is the same approach that Ladanyi and co-workers used to study mixtures of water and methanol,²⁶ and that Skaf recently used to study mixtures of DMSO and water.^{18,19} Souaille and Smith have pointed out that not incorporating the induced dipoles in the simulation is unlikely to affect the molecular motions of the liquid significantly, but some motions may not be spectroscopically visible.³⁵ Thus, absorption features arising from translational motions will not appear in the calculated spectra, and the effect of interference between the permanent and the induced dipoles, which may contribute significantly to the spectra,^{32,35} will also not be apparent. Despite these shortcomings, the permanent dipole represents the largest contribution to the spectral density and should be broadly representative of motions occurring in the liquid, particularly as the induced dipoles have much the same dielectric relaxation as the permanent dipoles.²⁶

IV. RESULTS

A. Spectra

The experimental and simulated spectra of the neat liquids are shown in Fig. 1. The simulations reproduce the positions of the absorption maxima fairly well, although the absorption peaks occur at slightly lower frequencies in the simulations than in the experimental results. However, the magnitude of the simulated absorption is too low, especially below 300 cm⁻¹, possibly because induced dipoles are not incorporated in the calculation of the spectrum.³⁶ In consequence of this lack of quantitative agreement, the simulated spectra at low frequencies should be regarded only as a first approximation to the correct result. For methanol, the simulated spectra compare more favorably with the experimental results at higher frequencies.^{1,37} In this case, the magnitude of the absorption and the position of the maximum absorption are close to those found experimentally. However, the absorption band from the simulations is asymmetric, but it is symmetric in the experimental results, and the widths of the absorption differ slightly.

The simulated spectra of the mixtures are shown in Fig.

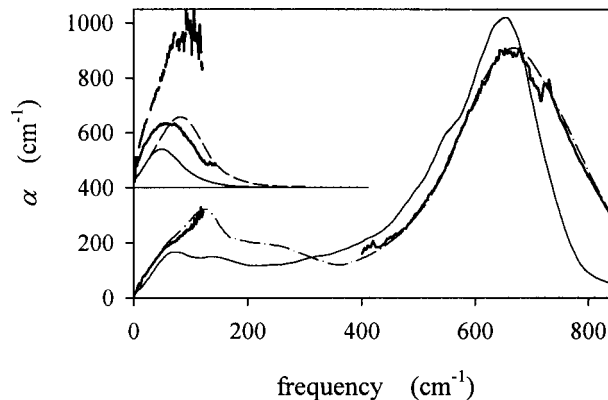


FIG. 1. Comparison of the experimental (bold lines) and simulated absorption spectra (thin lines) for the neat liquids. The absorption of methanol is shown as a solid line. For clarity, the absorption coefficients of acetone (solid line) and of acetonitrile (dashes) have been offset by 400 cm⁻¹. Experimental spectra are those determined in this work; Bertie's spectrum of neat methanol (thin dot-dashed line) is also shown (Ref. 37).

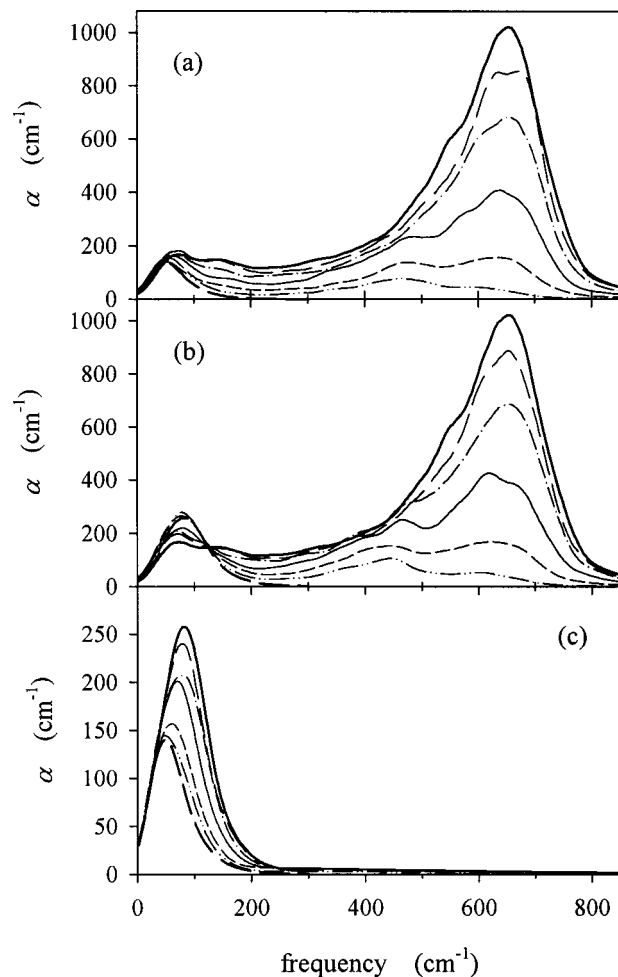


FIG. 2. Simulated absorption spectra of (a) acetone/methanol, (b) acetonitrile/methanol, and (c) acetone/acetonitrile mixtures. Bold and thin lines indicate neat liquids and mixtures, respectively. The compositions, by volume fraction of the first component, are 0.90 (dash-dot-dotted line), 0.75 (short dashes), 0.50 (solid line), 0.25 (dash-dotted line), and 0.10 (long dashes). The neat liquid of the first component is shown as bold dashes, the second component as a bold solid line.

2. The high frequency behavior of the acetone/methanol and acetonitrile/methanol mixtures is similar. Addition of acetone or acetonitrile to neat methanol brings about a decrease in the absorption coefficient around 650 cm^{-1} , as expected. However, as the concentration of the methanol in the mixture falls, a second feature begins to appear near 450 cm^{-1} . In both methanolic mixtures, this feature is of comparable magnitude to the 650 cm^{-1} peak at $V_{\text{ME}}=0.25$, and at $V_{\text{ME}}=0.10$ the lower frequency feature dominates the higher frequency peak. To estimate changes in the peak position and width, the first moment and the standard deviation of the absorption were calculated over the range $300\text{--}800 \text{ cm}^{-1}$. The results are shown in Fig. 3. Compositional trends in the experimental spectra are reproduced by the simulations: namely, a uniform decrease in peak position, and an increase in peak width that is reversed at low methanol concentrations. The lower value of the first moment of the absorption in the simulations is a result of the asymmetry of the high frequency spectrum: in neat methanol, the peak maximum of the simulated spectrum (ca. 650 cm^{-1}) is close to that of the

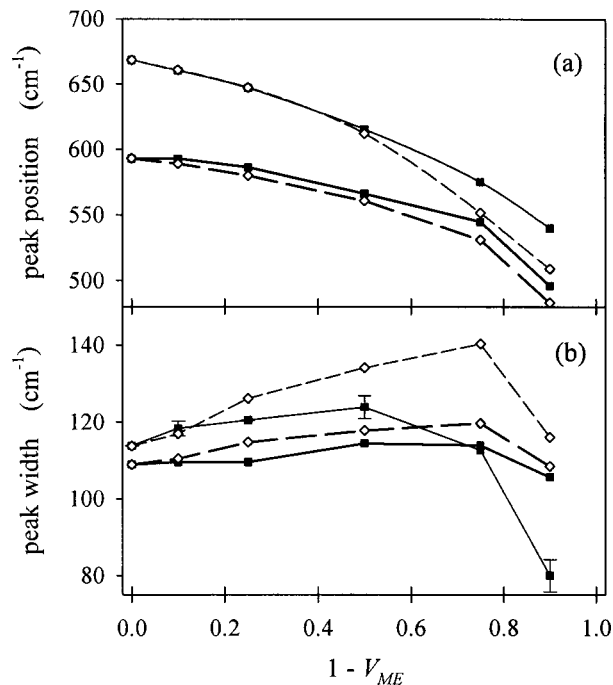


FIG. 3. Variation of the peak position (a) and width (b) of the high frequency methanol libration band as a function of the acetone or acetonitrile volume fraction. Thin lines denote values obtained by fitting the experimental absorption to a Gaussian curve, and bold lines represent the first moment and the standard deviation of the simulated spectra. Filled squares with solid lines indicate acetone/methanol mixtures, and open diamonds with dashed lines show acetonitrile/methanol mixtures. Uncertainties in the fits of the experimental data to a Gaussian are shown for the acetone/methanol mixtures.

experimental spectrum (670 cm^{-1}). The splitting of the absorption band results in a larger standard deviation of the absorption; thus, at low methanol compositions the high frequency peaks might be expected to have somewhat smaller widths than our calculation shows.

At low frequencies, the spectra of the methanolic mixtures show a relatively small excess absorption as the composition varies from neat methanol to neat acetone or acetonitrile (Fig. 4). The excess absorption is usually less than about 20 per cm, which may be large enough to be observed experimentally. However, our experimental far-IR spectra show no significant deviation from ideality. Above 100 cm^{-1} , the simulated spectra of the methanolic mixtures become more ideal. This is evident in the monotonic change in the absorption coefficient with composition, and in the isosbestic point at 125 cm^{-1} in the acetonitrile/methanol mixtures [Fig. 2(b)]. The spectra of mixtures of acetone and acetonitrile are essentially ideal at all the compositions considered.

More information on the particular molecular motions of each component in the liquid can be obtained from the ACFs of the single molecule dipole moment, as well as the linear and angular velocities, of each species. Ten molecules of each type were randomly chosen to calculate the single molecule ACFs. The velocity ACFs were evaluated for each molecular axis: for methanol, the molecule lies in the y - z plane and the z -axis is nearly parallel to the C-O bond. Two general observations can be made from evaluation of these func-

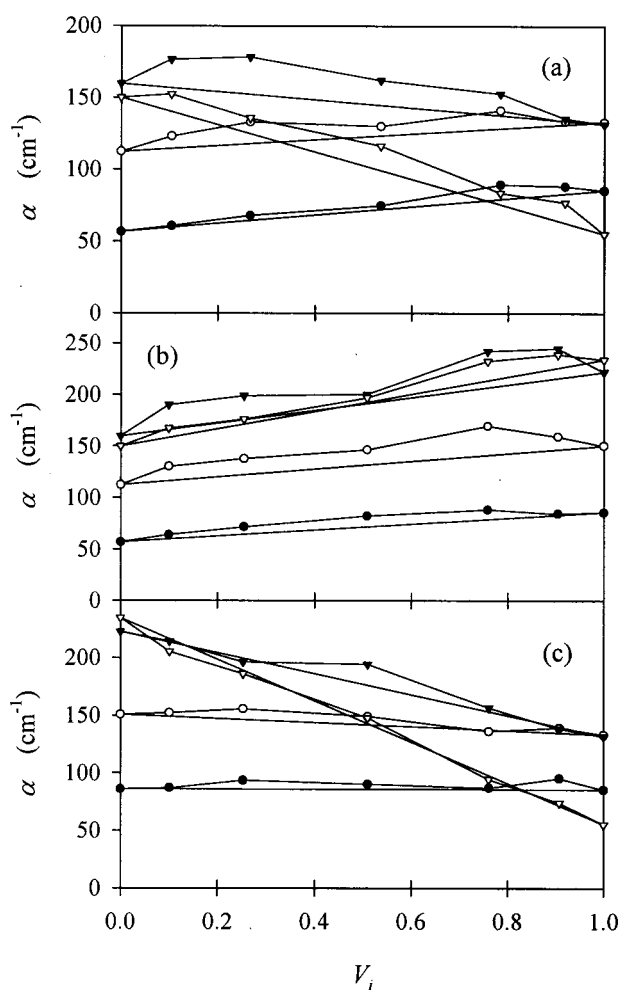


FIG. 4. Excess absorption of the simulated far-IR spectra of (a) acetone/methanol, (b) acetonitrile/methanol, and (c) acetone/acetonitrile mixtures. The volume fraction is in terms of the first component of the mixture. The frequencies shown are 20 cm^{-1} (filled circles), 40 cm^{-1} (open circles), 60 cm^{-1} (filled triangles), and 100 cm^{-1} (open triangles). Lines between adjacent points are meant as a guide to the eye. The ideal absorption is the line connecting the two neat liquids.

tions: (1) the largest changes occur in the motion of *methanol* molecules, and (2) that these changes are largest at *high frequencies*. Representative angular velocity and dipole ACFs and spectra of the mixtures will be presented below.

Spectra of the single dipole ACFs reveal information about the motion of individual molecules, as opposed to the collective motion in the liquid, which is described by the total dipole moment ACF. The single dipole spectra of methanol in both acetone and acetonitrile mixtures show a red-shift of the high frequency spectral density (Figs. 5 and 6). In acetonitrile/methanol mixtures, an isosbestic point is apparent at about 510 cm^{-1} , which strongly suggests a two-state system. The single dipole spectrum of methanol in acetone is similar to that in acetonitrile, but does not have a clear isosbestic point, possibly because the position of the lower frequency feature varies with acetone concentration. The lower frequency peak in these mixtures is found at slightly higher frequencies than in acetonitrile/methanol mixtures. In both mixtures, the spectral density below about 250 cm^{-1} decreases as methanol is diluted by cosolvent.

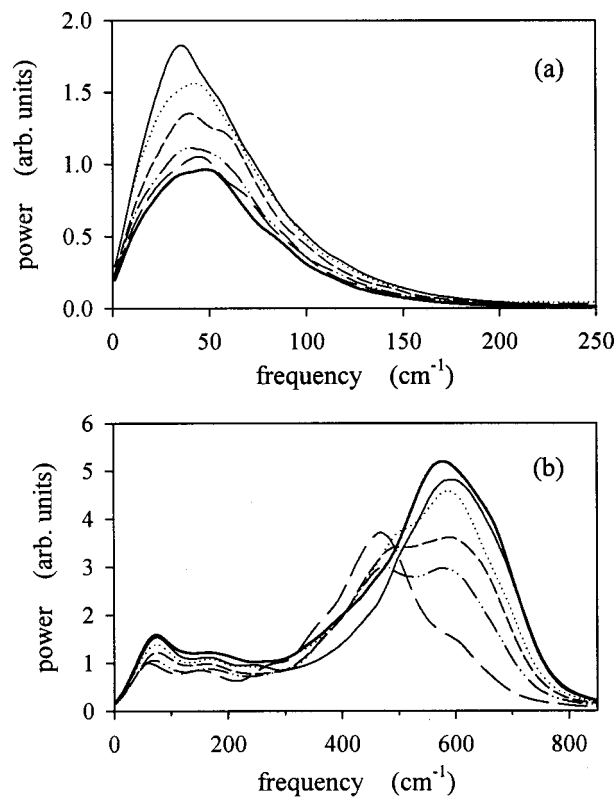


FIG. 5. The single dipole spectra of (a) acetone and (b) methanol in acetone/methanol mixtures. The bold solid line is the spectrum in the neat liquid, and thin lines show the spectra at the following volume fractions of acetone: 0.10 (solid line), 0.25 (dotted line), 0.50 (short dashes), 0.75 (dash-dot-dotted line), and 0.90 (long dashes).

The single dipole spectra of acetone and of acetonitrile in the methanolic mixtures both show an increase in spectral density in going toward methanol-rich compositions. This is accompanied by a red-shift in the peak position of the acetonitrile single dipole spectrum, from 64 cm^{-1} in neat acetonitrile to about 47 cm^{-1} at $V_{\text{AT}}=0.10$ (in acetonitrile/methanol mixtures). The red-shift in the acetonitrile mixtures is consistent with the results of Kovacs and Laaksonen for mixtures of acetonitrile and water.¹⁶ In acetone/acetonitrile mixtures, the single dipole spectral density of acetone increases slightly on addition of acetonitrile, whereas that of acetonitrile decreases somewhat and the peak position undergoes a small shift to lower wavelengths.

Autocorrelation functions of the linear velocities of each species and their corresponding spectra show little dependence on composition. Their linear motion is typically diffusive in the neat liquids, and addition of co-solvent tends to make them slightly slower and even more diffusive. These changes are reflected in small shifts of the spectral densities to lower frequencies.

Larger changes are observable in the angular velocities of acetonitrile and methanol as the neat liquids are diluted with co-solvent. The angular velocity ACFs show significant oscillatory behavior, which in the case of the methanol is very pronounced (Fig. 7). The angular velocity of acetonitrile slows on addition of co-solvent—this effect is slight where acetone is added to the mixture, but is much larger in methanol mixtures. Acetonitrile/methanol mixtures show a

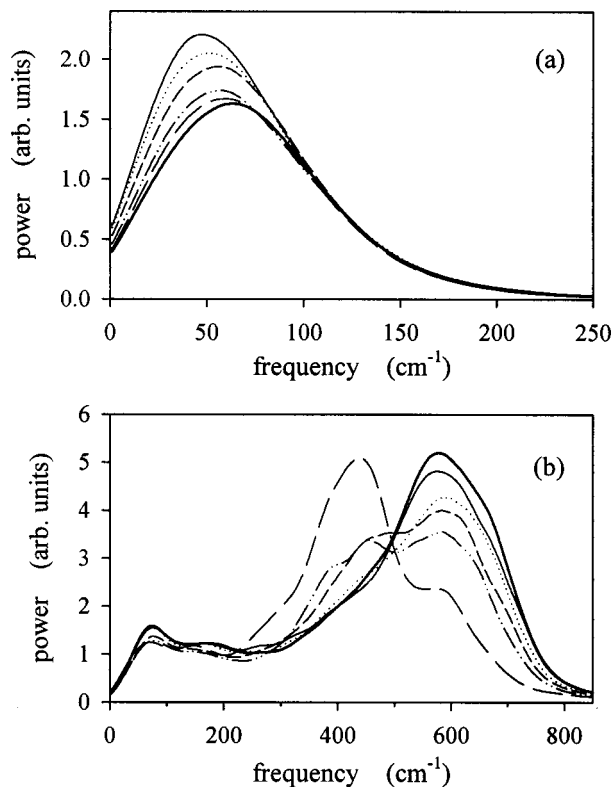


FIG. 6. Same as for Fig. 5, but for (a) acetonitrile and (b) methanol in acetonitrile/methanol mixtures.

large red-shift in the peak position, from about 60 cm^{-1} (neat acetonitrile) to 41 cm^{-1} for $V_{\text{ME}}=0.90$. In contrast, the angular velocities of acetone do not change much with composition.

The angular velocity ACFs of methanol are highly oscillatory, especially the ω_x and ω_z components, which correspond to rotation in the molecular plane and around the C–O axis, respectively. Spectra of these functions indicate the origin of features in the total dipole spectra. Thus, the high frequency absorption band has been assigned to libration of the hydroxyl H atom (ω_z), and the smaller absorption features at about 70 and 150 cm^{-1} (in neat methanol) arise from librations about the ω_y and ω_x axes, respectively. Because the I_{xx} and I_{yy} moments of inertia of methanol are so similar ($I_{yy}/I_{xx}=0.96$), differences in the frequencies of the corresponding librations must be attributed to a higher barrier for in-plane rotation (ω_x) than for out-of-plane rotation (ω_y).

The ω_x and ω_y motions are not much affected by acetone or acetonitrile, except in dilute mixtures when a narrowing and red-shift of the absorption band is observed. The motion most affected by composition is the angular velocity associated with rotating the hydrogen atom around the CO axis (ω_z). The most marked changes are seen in dilute methanol mixtures ($V_{\text{ME}}<0.50$). This motion is responsible for the prominent features observed in the total dipole and in the methanol single dipole spectra. The spectral density for this motion shows a lower frequency peak growing in at about 470 cm^{-1} in acetone and at 430 cm^{-1} in acetonitrile. The clear isosbestic points in each system again suggest a two-state system.

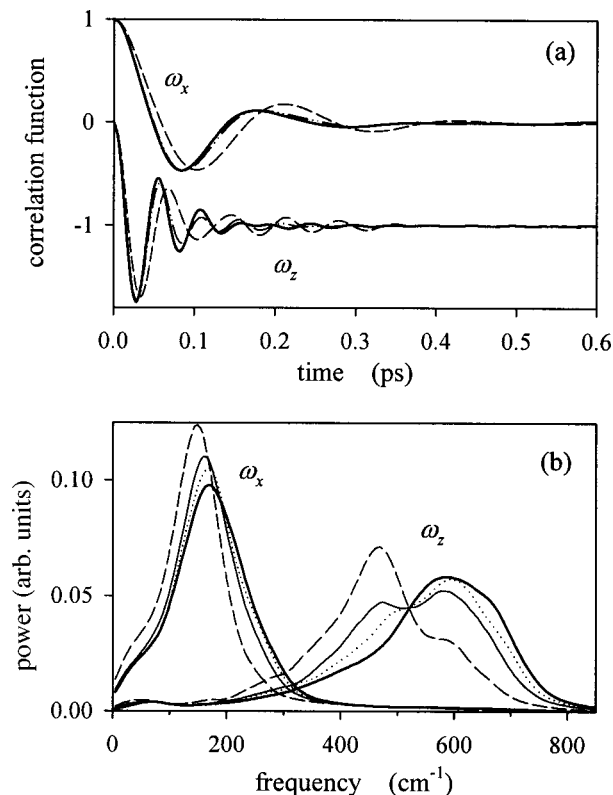


FIG. 7. The ACFs (a) and corresponding spectra (b) of the angular velocities ω_x and ω_z of the methanol molecule when mixed with acetone. (The coordinate system of the methanol molecule is described in the text.) ACFs are displayed for neat methanol (bold lines), and for mixtures of 0.50 (thin dash-dot-dotted line) and 0.90 (thin dashes) volume fraction acetone. In the graph of the spectra, neat methanol is again a bold solid line, and the mixtures shown are: 0.25 (thin dotted lines), 0.75 (thin solid line), and 0.90 (thin dashes), by acetone volume fraction.

B. Radial and spatial distribution functions

RDFs for the neat liquids agree with the literature results presented in Sec. II. Representative RDFs of the mixtures are shown in Fig. 8 to illustrate changes in the structure of the liquids upon mixing. The RDFs show that adding a co-solvent to either acetone or acetonitrile does not significantly affect the radial arrangement of these molecules among themselves [Figs. 8(a) and 8(b)]. An exception is that dilute mixtures of acetone or acetonitrile with methanol ($V_{\text{ME}}=0.90$) exhibit modest changes in the acetone–acetone and acetonitrile–acetonitrile RDFs in the direction of decreased structure. It seems reasonable to conclude from the above RDFs that, in mixtures, acetone molecules remain spatially unstructured relative to each other, and acetonitrile molecules show the same tendency for antiparallel alignment as they do in the neat liquid.^{11–13} Changes in the structure of acetone/acetonitrile mixtures are negligible.

In contrast to acetone and acetonitrile, RDFs indicating hydrogen bonding between methanol molecules undergo extraordinary changes as the methanol concentration decreases. Figures 8(c) and 8(d) show how the $\text{O}_{\text{ME}}-\text{O}_{\text{ME}}$ and $\text{O}_{\text{ME}}-\text{H}_{\text{ME}}$ RDFs increase as the methanol concentration decreases in acetone/methanol mixtures. The corresponding RDFs in the acetonitrile/methanol mixtures are essentially identical, excepting a slightly lower first maximum. These

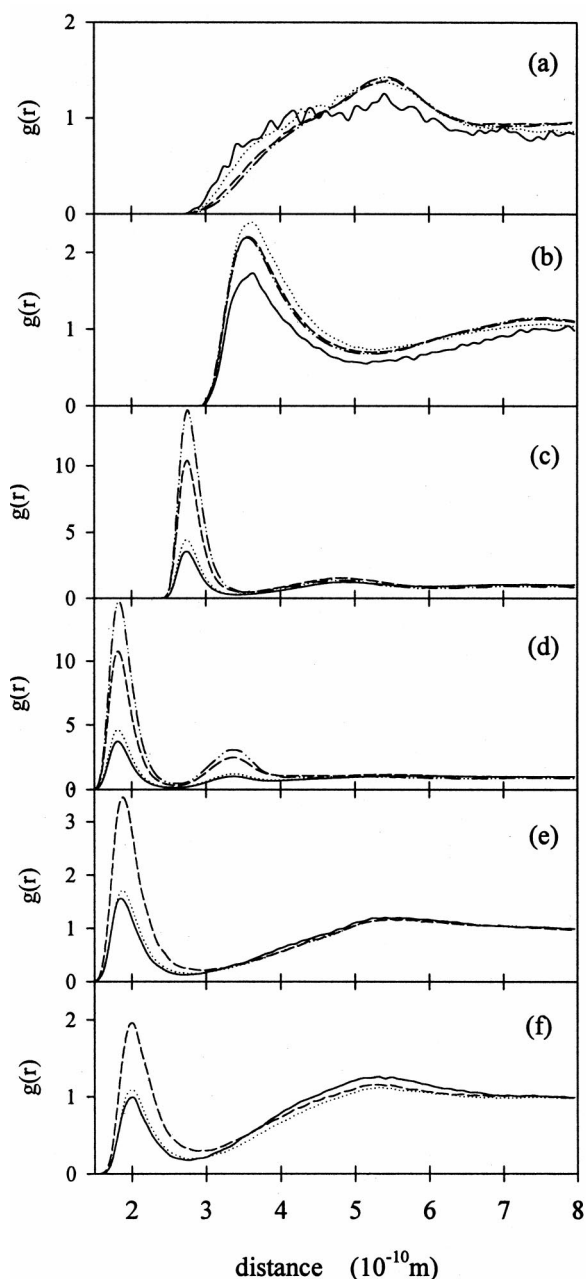


FIG. 8. RDFs of the following: (a) $O_{AT}-O_{AT}$ in acetone/methanol mixtures ($V_{AT}=0.10, 0.25, 0.75, 1.00$); (b) $N_{AN}-(CH_3)_{AN}$ in acetonitrile/methanol mixtures ($V_{AN}=0.10, 0.25, 0.75, 1.00$); (c) $O_{ME}-O_{ME}$ in acetone/methanol mixtures ($V_{AT}=0.00, 0.25, 0.75, 0.90$); (d) $O_{ME}-H_{ME}$ in acetone/methanol mixtures ($V_{AT}=0.00, 0.25, 0.75, 0.90$); (e) $O_{AT}-H_{ME}$ in acetone/methanol mixtures ($V_{AT}=0.10, 0.50, 0.90$); and (f) $N_{AN}-H_{ME}$ in acetonitrile/methanol mixtures ($V_{AN}=0.10, 0.50, 0.90$). The compositions, in the order listed, are shown as solid, dotted, dashed, and dash-dot-dotted lines.

results are indicative of the strong tendency of methanol molecules to self-associate through hydrogen bonding.

Hydrogen bonding interactions between methanol molecules and acetone or acetonitrile molecules are shown in Figs. 8(e) and 8(f) for the $O_{AT}-H_{ME}$ and $N_{AN}-H_{ME}$ RDFs. The distances of the peak maxima show that hydrogen bonds between methanol and acetone molecules are shorter than those between methanol and acetonitrile molecules. This result is expected from the smaller diameter of the hydrogen bond accepting sites: 2.96 Å (O_{AT}) versus 3.20 Å (N_{AN}). The

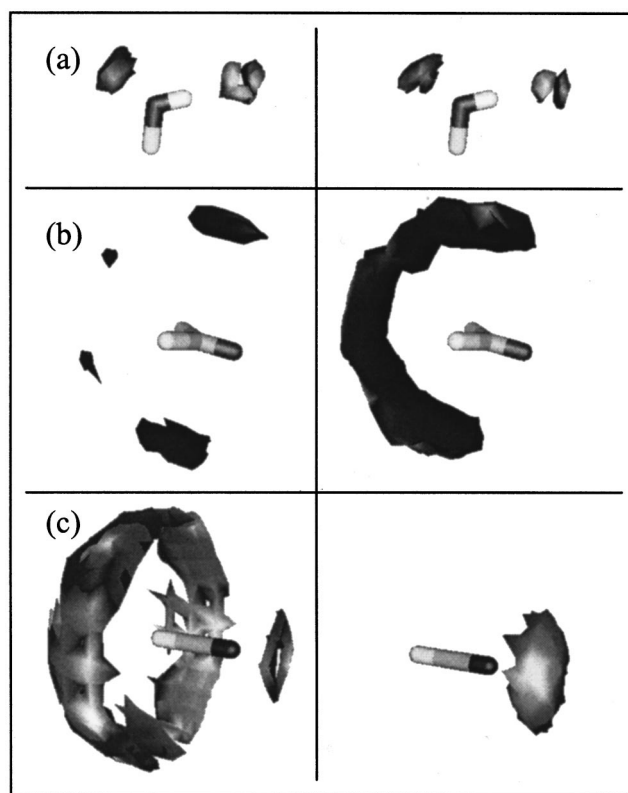


FIG. 9. SDFs of the (a) methanol, (b) acetone, and (c) acetonitrile molecules. The co-solvents in the above mixtures are acetone, methanol and methanol, respectively. The left panels show low concentrations of the central molecule ($V=0.10$), and the right panels are at high concentrations ($V=0.90$). The value of the plotted isosurface, a , and the overall maximum of the SDF, b , are denoted as (a/b). Values of a were chosen to highlight the qualitative trends without misrepresenting the results. In (a), SDFs between methanol and the H_{ME} are shown as dark surfaces, at (30/67) for low methanol concentrations and (10/22) for high concentrations (note that there are two H_{ME} maxima). Light surfaces in the methanol SDFs designate O_{ME} isosurfaces, at (70/111) and (30/70) for low and high concentrations, respectively. (b) shows SDFs between acetone molecules and O_{AT} , at (2.0/2.9) for low acetone concentrations and at (1.5/3.1) for high acetone concentrations. Panel (c) shows SDFs between the acetonitrile molecule and H_{ME} , at (15/17) for low acetonitrile concentrations, and (18/35) for high concentrations. The nitrogen atom of acetonitrile is shown by the dark site in the central molecule.

increase in the first maximum upon dilution of methanol indicates that methanol molecules become more likely to hydrogen bond to acetone or acetonitrile molecules, as is reasonable. Nonetheless, it is clear that methanol molecules have a greater ability to accept hydrogen bonds than do acetone and acetonitrile molecules.

Although the RDFs identify the most obvious structural features in the mixtures, ambiguity still exists about the exact location of sites relative to the central molecule. For instance, it is not clear whether the second maximum in the $N_{AN}-H_{ME}$ RDFs [Fig. 8(f)] arises from methanol molecules in a second solvent shell, or from a second preferential position for the hydrogen atom about the acetonitrile molecule. We therefore evaluated the spatial distribution functions (SDFs) of these mixtures because they complement the picture of the liquid structure obtained from the RDFs.³⁸ SDFs permit us to determine the most probable spatial location of a given site around the central molecule. Figure 9 shows the

SDFs of the mixtures at both ends of their composition range.

The location of methanol molecules relative to each other does not change significantly with composition [Fig. 9(a)], although the magnitude of the SDFs becomes exceptionally large at the hydrogen bonding positions as the methanol concentration decreases. The two prominent positions of neighboring methanol molecules are in the hydrogen bond donor and acceptor positions. The central methanol molecule donates an H atom directly toward the O atom of the hydrogen bond accepting neighbor. Another methanol molecule, which donates a hydrogen bond to the central molecule, is located near the bisector of the $\text{CH}_3\text{-O-H}$ angle. In a similar manner, the most likely position of the O_{AT} and N_{AN} atoms is in the hydrogen bond accepting position, but is not shown in Fig. 9(a).

The location of acetone and acetonitrile molecules relative to themselves in methanolic mixtures is affected by the composition. Figure 9(b) shows that in methanol-rich mixtures, acetone oxygen atoms lie above the plane of the central acetone molecule, whereas in acetone-rich mixtures, they occupy a broad crescent behind the central acetone molecule. This behavior is not obvious from Fig. 8(a), although the origin of the peak at 5.4 \AA in that figure immediately becomes clear after examining the associated SDF. Similarly, the cause of the second maximum in the $\text{N}_{\text{AN}}\text{-H}_{\text{ME}}$ RDFs [Fig. 8(f)] becomes apparent in the corresponding SDF [Fig. 9(c)]. It arises from the ringlike distribution of the H_{ME} atom around the acetonitrile molecule. The relative lack of preference for hydrogen bonding at low acetonitrile concentrations suggests that acetonitrile molecules are interspersed between methanol chains. At high acetonitrile concentrations, when the methanol chains have been broken up, there is relatively more hydrogen bonding between methanol and acetonitrile. Furthermore, SDFs show that the dipoles of both acetone and acetonitrile molecules point toward the H atom of methanol (not shown).

C. Hydrogen bonding and methanol chains

The hydrogen bonding state of molecules in methanolic mixtures has been assessed to clarify relationships between molecules in the mixture. Hydrogen bonds were evaluated according to the usual geometric criteria:^{6,21} for hydrogen bond accepting atom, Z, a hydrogen bond was assigned if $r_{\text{Z-H}} < 2.6 \text{ \AA}$, $r_{\text{Z-O}} < 3.5 \text{ \AA}$, and the $\text{H-O}\cdots\text{Z}$ angle was less than 30° . These values correspond approximately to the first minimum of the appropriate RDF of the system being studied. Using these criteria, our results for the number of hydrogen bonds in neat methanol were in excellent agreement with those of other workers.⁴⁻⁶ We have extended our analysis beyond counting the total number of hydrogen bonds per molecule by assessing the number of bonds donated and accepted by each molecule. In addition, hydrogen bonds donated were also categorized according to the recipient species. For brevity, the bonding state of methanol molecules is denoted by $n_D D_X - n_A A$, where n_D is the number of hydrogen bonds donated (0 or 1) to species X, and n_A is the number of hydrogen bonds accepted (0-2). Acetone and acetonitrile

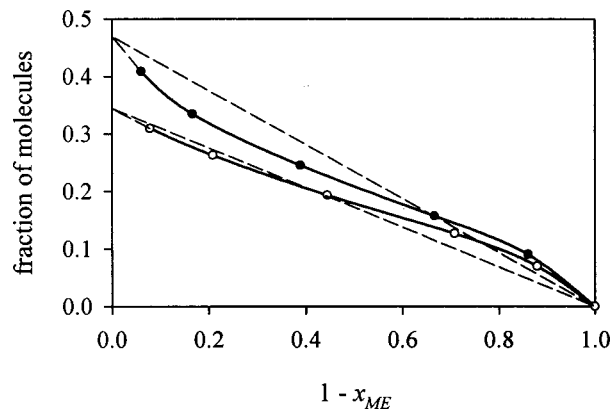


FIG. 10. The fraction of acetone molecules (filled circles) and acetonitrile molecules (open circles) which accept a hydrogen bond. The thin dashed line is the ideal curve, and the thick curve is meant as a guide to the eye.

trile molecules were recipients of either 0 or 1 hydrogen bond—there were negligibly few double hydrogen bond acceptors for these species.

The fraction of acetone and acetonitrile molecules involved in hydrogen bonding is shown in Fig. 10. The greater tendency for acetone than for acetonitrile to accept hydrogen bonds from methanol is evident at all compositions. Invoking the concept of ideality (dashed line in Fig. 10), the behavior of the two species is somewhat different. When infinitely diluted in methanol, acetone molecules are more likely (ca. 50%) than acetonitrile (ca. 34%) to be acceptors of a hydrogen bond. As the methanol mole fraction decreases, however, the probability of being hydrogen bonded converges to zero for both species. Furthermore, this probability is higher than ideal at low methanol concentrations, especially in acetonitrile/methanol mixtures.

The composition dependence of hydrogen bonding in methanol molecules is shown in Fig. 11 for acetonitrile/methanol mixtures. The results for acetone/methanol mixtures are similar. In neat methanol, most molecules are $1D_{\text{ME}}-1A$ —that is, middle-of-chain molecules—and a smaller proportion are chain-starting molecules ($1D_{\text{ME}}-0A$). Relatively few molecules are chain branches ($1D_{\text{ME}}-2A$). The number of hydrogen atoms not involved in hydrogen bonding is small, and includes free methanol molecules ($0D-0A$), and “dangling-hydrogen” chain-end molecules ($0D-1A$). The addition of acetonitrile makes possible two more bonding types, $1D_{\text{AN}}-0A$ and $1D_{\text{AN}}-1A$, corresponding, respectively, to methanol-acetonitrile dimers and to chain-ends terminating into acetonitrile molecules.

The hydrogen bonding of methanol molecules departs substantially from ideality as methanol is diluted by acetonitrile. Molecules taking part in chain formation ($1D_{\text{ME}}-0A$, $1D_{\text{ME}}-1A$, $0D-1A$, $1D_{\text{AN}}-1A$) have a convex curve as a function of composition, whereas nonchain methanol molecules have a concave dependence on composition. These observations demonstrate the strong propensity for methanol molecules to reside in chains. At the same time, it is apparent that the chains themselves must be disrupted and shortened, based on the increase in the fraction of metha-

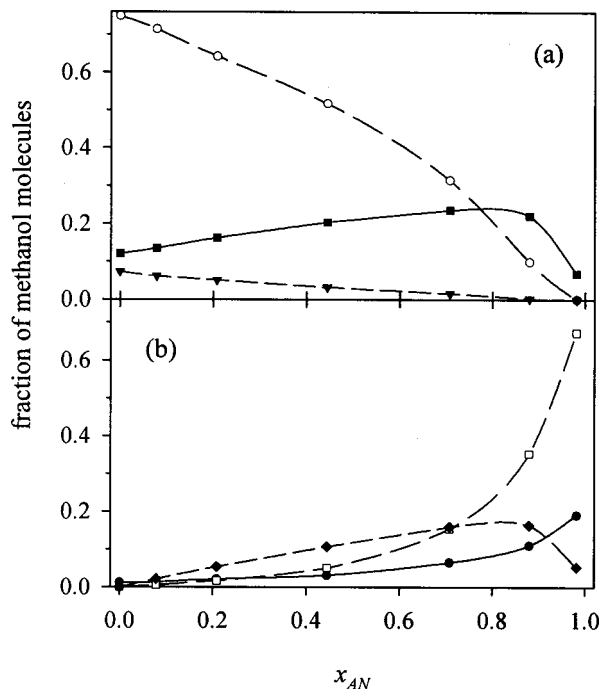


FIG. 11. The fraction of methanol molecules in different bonding states as a function of composition. The molecules shown in (a) are $1D_{ME-1A}$ (open circles) and $1D_{ME-0A}$ (filled squares), as well as methanol molecules that accept two hydrogen bonds (filled triangles). Molecules shown in (b) are $1D_{AN-0A}$ (open squares), $1D_{AN-1A}$ (filled diamonds), and $0D-0A$ (filled circles). We have incorporated the results of a simulation of methanol in acetonitrile-rich mixture ($V_{AN}=0.99$).

nol molecules at the start ($1D_{ME-0A}$) and at the end ($1D_{AN-1A}$ and $0D-1A$) of chains. Branching in chains gradually disappears, probably because of greater separation between chains. Thus, dangling-hydrogen chain-end molecules ($0D-1A$) would be less likely to meet up with other chains, which might thereby result in the coalescence of two chains into one larger (usually branched) chain.

The methanol chains were studied directly to verify the above points. Figure 12 shows how mixing affects the number of chains and the average number of methanol molecules per chain. (Acetone and acetonitrile molecules hydrogen bonded to the chain were not counted as part of the chain.) Our average chain length for neat methanol (16.5) is close to

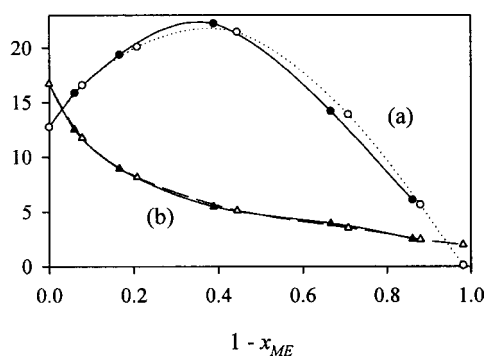


FIG. 12. The average number of chains (a), and the average number of methanol molecules per chain (b), as a function of the mole fraction of acetone or acetonitrile. Lines connecting points are included to guide the eye.

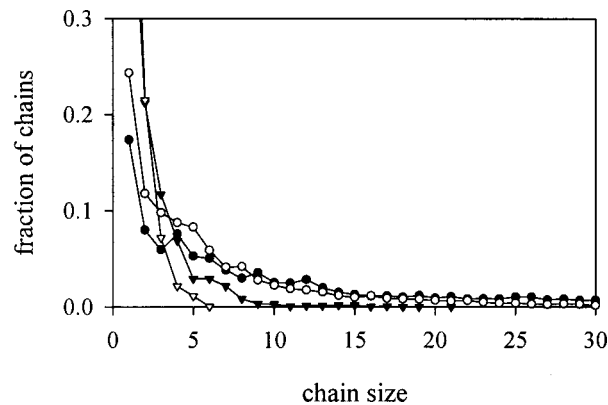


FIG. 13. The chain size distribution in acetonitrile/methanol mixtures the following compositions: $V_{AN}=0.90$ (open triangles), $V_{AN}=0.75$ (filled triangles), $V_{AN}=0.25$ (open circles), and neat methanol (filled circles).

the value obtained by Matsumoto and Gubbins (15.5).⁵ The number of chains in the liquid increases on adding acetone or acetonitrile, resulting in a maximum near $x_{ME}=0.6$. The greater number of chains occurs despite fewer methanol molecules in the mixture. A rapid decrease in chain size accompanies the increase in number of chains—the average number of methanol molecules per chain is halved upon addition of 0.2 mole fraction co-solvent—and is followed by a slower decrease in chain size as further solvent is added. The distribution of chain lengths in acetonitrile/methanol mixtures is shown in Fig. 13. There is a clear shift toward shorter chains as more acetonitrile is added. The largest changes are apparent in the $V_{ME}=0.25$ and 0.10 mixtures, in which almost all chains have fewer than five molecules.

An interesting issue concerns the shapes of the methanol chains, and how they are affected by mixing. To explore this point, we calculated the moments of inertia of the chains based on the center-of-mass of the constituent molecules. The smallest principal moment of inertia for a chain was assigned as I_{xx} , the intermediate as I_{yy} , and the largest moment as I_{zz} . Ratios of the average moments of inertia (I_{xx}/I_{yy} and I_{yy}/I_{zz}) according to chain size are plotted in Fig. 14. The chains tend to have a prolate shape, with the

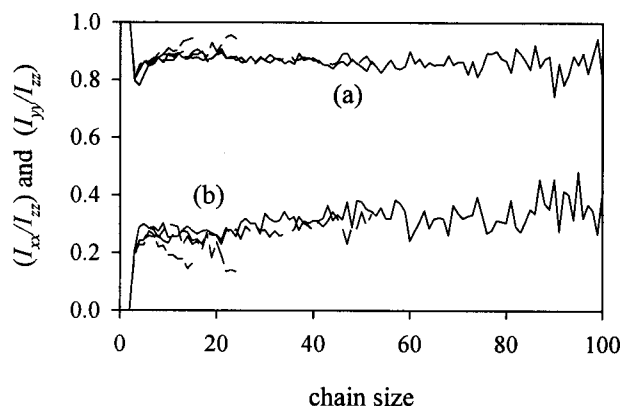


FIG. 14. The effect of methanol chain size on the ratios of the average moments of inertia of the chains in acetone/methanol mixtures. Compositions shown are neat methanol (solid line), $V_{AT}=0.25$ (long dashes), $V_{AT}=0.50$ (medium dashes), and $V_{AT}=0.75$ (short dashes).

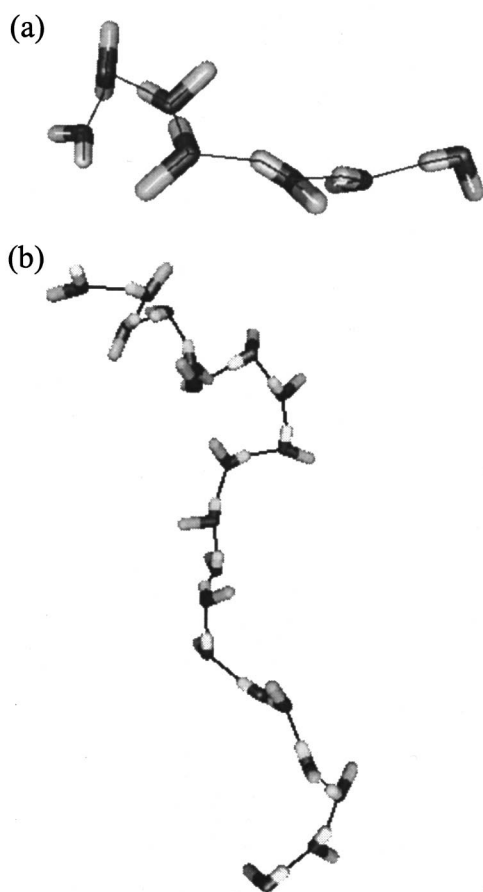


FIG. 15. Example configurations of methanol chains, showing the twisting of the chains. The oxygen atom is shown by the dark site, and the hydrogen is the lightest site. Hydrogen bonds are shown by thin lines connecting hydrogen and oxygen atoms of adjacent molecules. (a) and (b) have 7 and 20 molecules in the chain, respectively.

moment of inertia about the x axis roughly three times smaller than about the other axes. The I_{xx}/I_{zz} and I_{yy}/I_{zz} values are stable with increasing chain length, as entropy favors clusters that are stretched out over structures that are more spherical. Addition of acetone or acetonitrile appears to have little effect on the I_{xx}/I_{zz} and I_{yy}/I_{zz} ratios, although at low methanol concentrations there may be a slight tendency for the chains to become even more stretched out (see I_{xx}/I_{zz} for $V_{AT}=0.75$ and 0.90).

The configurations of many chains of different lengths were examined. Most chains conformed to the shape expected from Fig. 14; that is, they tended to be somewhat elongated, with approximately equal distributions off the major axis. Two representative configurations of chains are shown in Fig. 15. Bunching of the chains into spherical clusters was rarely seen. There is a pronounced tendency for segments of the chain to curl gently, which was usually associated with methyl groups of adjacent molecules being in an eclipsed position (on the outside of the curve). A consequence of the curling is that chains often have a helical character. In some cases, methyl groups of adjacent molecules were staggered, resulting in straighter chain segments. When branching occurred, it was usually near the end of the chains.

There were no noticeable differences between the conformations of chains in neat methanol and those in mixtures.

V. DISCUSSION

Translational and rotational motions that cause dipole fluctuations are responsible for the intermolecular infrared spectra of liquids. Rotational motion usually reorients the permanent dipole of a molecule, and hence gives rise to strong infrared absorption. Translational motions contribute to the absorption by modulating the induced dipoles between molecules. Translational motions will not be spectroscopically active in our simulated spectra, because we have not incorporated induced dipoles (either dipole-induced or collision-induced) into our study. However, for molecules with large permanent dipoles, such as those considered in this study, rotational motions are responsible for most of the infrared absorption.

Comparison of the experimental and the simulated spectra reveals that the simulations underestimate the absorption of the liquids at low frequencies. Although the peak positions of the acetone and acetonitrile spectra were close to the experimental results, the magnitude of the predicted absorption coefficients was too low. This shortfall is partly due to the absence of induced dipoles in the calculated spectra,^{7,36} but may also result from inaccuracies in the effective potential.

The simulated spectra reproduce the ideal behavior found in the experimental spectra of acetone/acetonitrile mixtures. The simulations also indicate that in this system there is little change in the librational and translational motions of each species as a function of composition. Therefore, at least with regard to these motions, acetone/acetonitrile mixtures appear to behave ideally.

The agreement between trends in the simulated and experimental spectra of methanolic mixtures was not as satisfactory as in the acetone/acetonitrile mixtures. The composition of the mixtures does not affect the translational motions of each component in a significant way. For methanol molecules, this is in accordance with the work of Martí *et al.*, who have previously shown that the hydrogen bonding state of methanol molecules has little effect on the translational motion below 100 cm^{-1} .⁶ However, the librational motions of both species are shifted to lower frequencies, giving rise to a small excess absorption in the low frequency spectra of the mixtures, which is not observed experimentally. The behavior of the ideal experimental absorption of methanolic mixtures may be due to a cancellation effect between the red-shift of the librational motions, and a decrease in the absorption from the Debye relaxation, which is the primary cause of the nonideal absorption of aqueous mixtures. However, we emphasize that the observed nonidealities in the simulated spectra are quite small. Reasons for the dissimilarity in the far-IR spectra of aqueous and methanolic mixtures have been discussed in the preceding paper.¹

The simulated spectra of methanolic mixtures reproduce the most prominent changes in the high frequency librational band of methanol. The peak position of neat methanol is close to the experimental value, and both mixtures result in a red-shift which is similar to that seen in the experimental

spectra. At low methanol concentrations, the simulated librational absorption band splits into two peaks, but the experimental spectra show no evidence for splitting of the peak. Similar behavior has been reported by Skaf in simulations of water–DMSO mixtures.^{18,19} We measured the absorption spectrum of this system at the same concentration as their study ($x_{\text{DMSO}}=0.84$). Although the high frequency librational band did shift to lower frequencies (as predicted by the simulations), there was no experimental evidence for splitting of the peak.

Changes in the librational motion of the methanol molecule about the z axis are responsible for the behavior of the high frequency spectra. A striking feature is the appearance of an isosbestic point in the methanol ω_z spectra for both mixtures, which suggests a two-state system. Because the largest intermolecular interaction that the methanol molecule experiences is from hydrogen bonding, the two-state nature of the ω_z motion is probably due to different hydrogen bonding environments. The work of Matsumoto and Gubbins suggests that methanol molecules involved in 1 to 3 hydrogen bonds have similar ω_z librational frequencies, which are substantially higher than those of nonbonded methanol molecules. We propose that the high frequency motion occurs in hydrogen bond *donating* molecules, and involves rotation of the hydrogen atom through the hydrogen bond. The higher frequency of libration is then caused by the strong restoring force between the hydrogen atom and the hydrogen bond accepting atom. Methanol molecules with nonbonded hydrogen atoms therefore librate at lower frequencies, as do those with weaker hydrogen bonds to acetone or acetonitrile. The number of methanol molecules donating a hydrogen bond to acetone or acetonitrile increases sharply at low methanol concentrations, which corresponds to the appearance of the lower frequency peak. Therefore, it seems reasonable to attribute the low frequency peak to hydrogen bonding between methanol and acetone or acetonitrile, instead of to nonbonded methanol molecules, which never exist in large numbers in the mixtures.

The broadening of the high frequency absorption band on dilution of methanol arises from methanol molecules adopting a more diverse range of hydrogen bonding states. In neat methanol, 75% of molecules are in the middle of chains ($1D_{\text{ME}}-1A$), but addition of a co-solvent shortens the chains, to give more molecules at the ends of chains and fewer middle-of-chain molecules. This trend increases with further dilution, until low methanol concentrations, when most methanol molecules are hydrogen bonded to the co-solvent. Consequently, the environment of methanol molecules is somewhat more homogeneous at low methanol concentrations than at intermediate concentrations, as indicated by the narrower frequency band. Palinkas *et al.* have interpreted the broadening of the spectra of water/methanol mixtures in a similar manner.³⁹

The simulations appear to under-represent the number of hydrogen bonds accepted by acetone and acetonitrile in the mixtures. The experimental results of Eaton *et al.* indicate that acetone or acetonitrile, when in methanol-rich mixtures, participate in almost twice as many hydrogen bonds as in our simulations (Fig. 10).^{39–42} Hydrogen bonding between ac-

etone or acetonitrile and methanol is thus stronger in real than in simulated mixtures.

The structure of acetone/acetonitrile mixtures, in which hydrogen bonding does not play a role, is almost unchanged upon mixing. There is no tendency toward self-association—molecules of either species are evenly distributed throughout the mixture. This comes as no surprise, as the structures of the neat liquids appear to be primarily determined by steric effects.¹³ Dipole–dipole interactions are somewhat less important, but do maintain the antiparallel alignment of acetonitrile molecules. The absence of strong, highly specific and directional interactions (such as hydrogen bonding) distinguishes this system from the methanolic mixtures.

In contrast to acetone/acetonitrile mixtures, large changes occur in the RDFs of methanolic mixtures. The most prominent changes appear in the RDFs associated with hydrogen bonding and are similar to those that take place in aqueous mixtures. The increases in the hydrogen bonding RDFs between methanol molecules are not so much caused by an increase in the structure of methanol, as they are by the tendency of methanol to remain in chains in mixtures. Even at low methanol concentrations, most methanol molecules reside in chains. Thus, for any given methanol molecule, there is always a high probability of finding another methanol molecule as a neighbor, irrespective of whether the overall methanol concentration is high or low. The ability of methanol to form chains is probably due to the stability of methanol molecules with two hydrogen bonds.⁵ Because there is no strong force drawing them together, acetone or acetonitrile molecules tend to be evenly dispersed throughout the mixture at high methanol concentrations.

Adding acetone or acetonitrile to methanol breaks up large chains into smaller and more numerous chains. The shapes of the chains are little affected by mixing and the helical, prolate character of the chains is retained. At low methanol concentrations, however, the occurrence of methanol-acetone and methanol-acetonitrile dimers increases considerably. The strong tendency of methanol to donate hydrogen bonds is extraordinary, and few hydrogen atoms do not participate in hydrogen bonding. Hydrogen bonds formed between methanol molecules are stronger than methanol-acetone or methanol-acetonitrile hydrogen bonds.

VI. CONCLUSIONS

Spectra based on MD simulations of binary mixtures containing methanol, acetone, and acetonitrile were compared to the experimental results of the preceding paper. Simulated spectra reproduce the ideal behavior of the acetone/acetonitrile mixtures, but show a small excess absorption of methanolic mixtures in the far-IR, arising from a red-shift of the methanol and acetonitrile librational bands. The far-IR spectra of methanolic mixtures contrast with those of aqueous mixtures, which we have also determined.^{25,27} Aqueous mixtures show a decreased absorption compared to ideal mixtures. Explanations for the dissimilar behavior were proposed in terms of changes in the reorientational motions in the mixtures.

Simulations reproduce the shape and trends of the high frequency librational band of methanol, which arises from

the librations of the hydroxyl hydrogen atom around the C–O bond axis. This band is therefore a sensitive indicator of the hydrogen bonding environment experienced by the methanolic molecule. The red-shift upon mixing is attributed to hydrogen bonding between methanol and acetone or acetonitrile. Methanol molecules have a remarkably strong tendency to remain in chains, although the chains shorten as the methanol concentration decreases. Chains were found to be prolate with helical regions, and their general structure is not significantly affected by concentration.

The effect of acetone and acetonitrile on methanol behavior is similar, despite significant differences in the size and dipole moments of the acetone and acetonitrile molecules. Clearly, their effect on methanol is through their ability to accept hydrogen bonds, which is the primary determinant of structure and dynamics in methanolic mixtures. Acetone/acetonitrile mixtures appear to behave ideally, in terms of both structure and of dynamics.

ACKNOWLEDGMENTS

Support from a National Science Foundation CAREER award (CHE-9703432) is gratefully acknowledged. We thank Allan Chiu for technical assistance.

- ¹D. S. Venables, A. Chiu, and C. A. Schmuttenmaer, *J. Chem. Phys.* **113**, 3243 (2000), preceding paper.
- ²E. Hawlicka, *Pol. J. Chem.* **70**, 821 (1996).
- ³W. L. Jorgensen, *J. Phys. Chem.* **90**, 1276 (1986).
- ⁴M. Haughney, M. Ferrario, and I. R. McDonald, *J. Phys. Chem.* **91**, 4934 (1987).
- ⁵M. Matsumoto and K. E. Gubbins, *J. Chem. Phys.* **93**, 1981 (1990).
- ⁶J. Martí, J. A. Padró, and E. Guàrdia, *J. Mol. Liq.* **64**, 1 (1995).
- ⁷M. S. Skaf, T. Fonseca, and B. M. Ladanyi, *J. Chem. Phys.* **98**, 8929 (1993).
- ⁸P. Jedlovszky and G. Pálinkás, *Mol. Phys.* **84**, 217 (1995).
- ⁹M. Ferrario, M. Haughney, I. R. McDonald, and M. L. Klein, *J. Chem. Phys.* **93**, 5156 (1990).
- ¹⁰W. L. Jorgensen, J. M. Briggs, and M. L. Contreras, *J. Phys. Chem.* **94**, 1683 (1990).
- ¹¹W. L. Jorgensen and J. M. Briggs, *Mol. Phys.* **63**, 547 (1988).
- ¹²T. Ohba and S. Ikawa, *Mol. Phys.* **73**, 999 (1991).
- ¹³T. Radnai and P. Jedlovszky, *J. Phys. Chem.* **98**, 5994 (1994).
- ¹⁴A. Laaksonen and P. Stilbs, *Mol. Phys.* **74**, 747 (1991).
- ¹⁵Y. P. Puhovski and B. M. Rode, *J. Chem. Phys.* **102**, 2920 (1995).
- ¹⁶H. Kovacs and A. Laaksonen, *J. Am. Chem. Soc.* **113**, 5596 (1991).
- ¹⁷D. A. Zichi and P. J. Rossky, *J. Chem. Phys.* **84**, 2814 (1986).
- ¹⁸I. A. Borin and M. S. Skaf, *Chem. Phys. Lett.* **296**, 125 (1998).
- ¹⁹M. S. Skaf, *J. Phys. Chem. A* **103**, 10719 (1999).
- ²⁰M. P. Allen and D. J. Tildesley, *Computer Simulation of Liquids* (Clarendon, Oxford, 1987).
- ²¹A. Luzar and D. Chandler, *J. Chem. Phys.* **98**, 8160 (1993).
- ²²H. Tanaka and K. E. Gubbins, *J. Chem. Phys.* **97**, 2626 (1992).
- ²³G. Pálinkás, E. Hawlicka, and K. Heinzinger, *Chem. Phys.* **158**, 65 (1991).
- ²⁴Y. P. Puhovski and B. M. Rode, *J. Phys. Chem.* **99**, 1566 (1995).
- ²⁵D. S. Venables and C. A. Schmuttenmaer, *J. Chem. Phys.* **108**, 4935 (1998).
- ²⁶B. M. Ladanyi and M. S. Skaf, *J. Phys. Chem.* **100**, 1368 (1996).
- ²⁷D. S. Venables and C. A. Schmuttenmaer (unpublished).
- ²⁸H. Kovacs, J. Kowalewski, and A. Laaksonen, *J. Phys. Chem.* **94**, 7378 (1990).
- ²⁹The MolDy program was coded by K. Refson, and can be downloaded from the internet at <http://www.earth.ox.ac.uk/%7Ekeith/moldy.html>
- ³⁰A. Bródka and T. W. Zerda, *J. Chem. Phys.* **104**, 6319 (1996).
- ³¹D. R. Lide, Ed., *CRC Handbook of Chemistry and Physics*, 73rd ed. (CRC Press, Boca Raton, 1992).
- ³²B. Guillot, *J. Chem. Phys.* **95**, 1543 (1991).
- ³³D. A. McQuarrie, *Statistical Mechanics* (Harper-Collins, New York, 1976).
- ³⁴A. Kramers–Kronig calculation requires the high frequency index of refraction. The indices of refraction for the neat liquids at 20 °C are 1.359 (acetone), 1.344 (acetonitrile), and 1.328 (methanol) (Ref. 31). Ideal values of the indices of refraction were used for the mixtures.
- ³⁵M. Souaille and J. C. Smith, *Mol. Phys.* **87**, 1333 (1996).
- ³⁶D. M. F. Edwards and P. A. Madden, *Mol. Phys.* **51**, 1163 (1984).
- ³⁷J. E. Bertie and S. L. Zhang, *J. Chem. Phys.* **101**, 8364 (1994).
- ³⁸A. Laaksonen, P. G. Kusalik, and I. M. Svishchev, *J. Phys. Chem. A* **101**, 5910 (1997).
- ³⁹G. Pálinkás, I. Bakó, K. Heinzinger, and P. Bopp, *Mol. Phys.* **73**, 897 (1991).
- ⁴⁰G. Eaton, A. S. Pena-Núñez, and M. C. R. Symons, *J. Chem. Soc., Faraday Trans. 1* **84**, 2181 (1988).
- ⁴¹G. Eaton, A. S. Pena-Núñez, M. C. R. Symons, M. Farrario, and I. R. McDonald, *Faraday Discuss. Chem. Soc.* **85**, 237 (1988).
- ⁴²M. C. R. Symons and G. Eaton, *J. Chem. Soc., Faraday Trans. 1* **81**, 1963 (1985).